Surface Functional Evolution of *Solanum rostratum* Biochars Regulates Sorption-Mediated Stabilization of Soil Organic Carbon and Microbial Assembly

Lei Song †, Peifeng Xu †, Xiaorong Zhang, Zongqiang Gong *

Posted Date: 19 November 2025

doi: 10.20944/preprints202511.1492.v1

Keywords: biochar; sorption mechanisms; adsorption; surface functional groups; soil organic carbon; carbon stabilization; microbial assembly processes; FTIR; XPS; pyrolysis temperature

 doi:10.20944/preprints202511.1492.v1

Article

Surface Functional Evolution of *Solanum rostratum* Biochars Regulates Sorption-Mediated Stabilization of Soil Organic Carbon and Microbial Assembly

Lei Song [1,2,†], Peifeng Xu [1,2,†], Xiaorong Zhang [1] and Zongqiang Gong [1,*]

[1] CAS Key Laboratory of Forest Ecology and Silviculture, Institute of Applied Ecology, Chinese Academy of Sciences, Shenyang 110016, China

[2] University of Chinese Academy of Sciences, Beijing 100049, China

* Correspondence: zgong@iae.ac.cn

† These authors contributed equally to this work.

Abstract

Biochar surface chemistry strongly influences the adsorption and partitioning of organic matter in soils, yet the sorption-mediated stabilization mechanisms of biochars derived from invasive plant biomass remain poorly constrained. In this study, *Solanum rostratum* biomass was pyrolyzed at 300–700 °C to generate biochars with distinct surface functionalities and structural characteristics. Multi-analytical characterization (FTIR, Raman, XPS, SEM) was used to quantify temperature-induced changes in aromaticity, oxygen-containing groups, and pore morphology, while soil incubation experiments assessed impacts on organic carbon fractions. High-temperature biochars showed reduced O-containing groups and enhanced aromatic condensation, indicating a shift from hydrogen bonding and electrostatic interactions to hydrophobic and π–π sorption mechanisms. These surface transformations were associated with increased stable carbon pools and reduced labile carbon in soil, consistent with stronger adsorption and protection of organic matter. Sequencing analysis revealed that biochar amendments significantly altered bacterial community composition and enhanced deterministic assembly processes, suggesting that microbial reorganization further reinforces sorption-driven carbon stabilization. These findings demonstrate that *S. rostratum* biochars possess strong sorptive properties that promote long-term carbon retention and modulate microbial ecological processes, supporting their potential use as sustainable adsorbents in soil carbon management.

Keywords: biochar; sorption mechanisms; adsorption; surface functional groups; soil organic carbon; carbon stabilization; microbial assembly processes; FTIR; XPS; pyrolysis temperature

1. Introduction

Soils constitute the largest terrestrial carbon (C) reservoir, storing more carbon than the atmosphere and vegetation combined [1]. Enhancing or preserving soil organic carbon (SOC) stocks is therefore crucial for sustaining soil fertility and mitigating climate change through long-term C sequestration. However, SOC is vulnerable to losses due to microbial mineralization and decomposition, particularly under anthropogenic pressure and environmental change [2,3]. Biochar, a carbon-rich material generated by pyrolyzing biomass under oxygen-limited conditions, has attracted significant attention as a soil amendment that can stabilize SOC while improving soil physicochemical and biological properties [4,5].

One of biochar's most compelling features is its adsorptive capacity, arising from its high surface area, porosity, and variable surface functional groups [6,7]. These properties allow biochar to sorb a wide range of organic molecules, including microbial exudates, root-derived compounds, and soluble nutrients, potentially modulating microbial access to labile substrates and influencing carbon

 doi:10.20944/preprints202511.1492.v1

turnover [8,9]. Recent studies have suggested that such "adsorptive filtering" effects may restructure microbial communities by altering niche availability, with consequences for ecosystem functions such as nutrient cycling and SOC stabilization [10].

Pyrolysis temperature plays a pivotal role in determining the physicochemical characteristics of biochar, including its sorption properties [11,12]. Low-temperature biochars (300–400 °C) tend to retain more polar surface groups and labile carbon, whereas high-temperature biochars (≥600 °C) are more aromatic, carbon-dense, and chemically stable but often lose reactive functionalities [13]. These transformations influence both the direct stability of biochar-C and its interactions with native soil organic matter and microbial populations [14]. Optimal pyrolysis conditions may therefore balance carbon recalcitrance and interactive capacity, producing biochars that can sequester carbon while actively participating in soil biogeochemical cycles [15,16].

Biochar's sorptive properties also offer a mechanistic link between its chemical structure and its effects on microbial community assembly [17,18]. For instance, biochar can adsorb extracellular enzymes, microbial signaling molecules, and toxins, thereby shaping microbial habitat quality [19]. This may lead to niche filtering, where only taxa capable of thriving under altered resource availability can persist, increasing deterministic processes in community assembly [20,21]. Quantitative ecological models using indices such as β-nearest taxon index (βNTI) and Raup–Crick dissimilarity provide tools to detect such assembly patterns and link them to underlying environmental drivers [22].

From a feedstock sustainability perspective, converting invasive or weedy plants into biochar represents a promising strategy. Invasive species such as *Solanum rostratum* produce abundant biomass and pose ecological threats to native ecosystems and agriculture [23,24]. Rather than being treated solely as waste, this biomass can be transformed into functional materials for environmental remediation, supporting circular economy principles and negative-emission strategies [25].

Despite the recognized benefits of biochar, relatively few studies have explicitly examined how biochar's adsorption-mediated effects shape microbial community structure and SOC stabilization, particularly when produced from invasive plant biomass [26]. Moreover, the interplay between biochar surface chemistry, microbial niche filtering, and the partitioning of SOC into labile and stable pools remains poorly understood [27]. Addressing this knowledge gap is essential for optimizing biochar design and deployment.

In this study, we investigated the effects of *S. rostratum*-derived biochars produced at three pyrolysis temperatures (400 °C, 500 °C, 600 °C) on soil carbon stability and microbial communities. We focused on how pyrolysis-induced variation in biochar sorptive properties influence microbial diversity, functional potential, and community assembly mechanisms. Simultaneously, we quantified carbon mineralization dynamics using a two-pool kinetic model to assess biochar's impact on labile versus stable SOC pools [28]. By integrating adsorption theory with microbial ecology and soil biogeochemistry, our work aims to elucidate the dual role of invasive-plant biochar as a carbon sink and microbial habitat modifier.

2. Materials and Methods

2.1. Soil and Biomass Sampling and Preparation

Soil samples were collected from riparian shelterbelts along the Daling River, western Liaoning Province, Northeast China (41°12′-41°18′ N, 120°39′-120°45′ E). The region features a semi-arid continental monsoon climate, with a mean annual temperature of approximately 8.5 °C and precipitation ranging from 450 to 550 mm, mostly concentrated between July and September. The soils, classified as sandy loam, are prone to aeolian erosion and are commonly utilized in protective afforestation projects under the Three-North Shelterbelt Program.

Aboveground biomass of the invasive species *Solanum rostratum* Dunal, commonly found on degraded riverbanks and abandoned farmland beneath shelterbelts, was harvested at full maturity in July 2023. The plant material was cut at the base, transported in sealed polyethylene bags, and

 doi:10.20944/preprints202511.1492.v1

washed thoroughly with tap water followed by distilled water to remove soil and debris. Samples were sun-dried for 7 days until constant weight, then ground using a high-speed mill and sieved to pass through a 0.25 mm mesh to ensure uniformity. The processed biomass was stored in airtight plastic containers at room temperature prior to pyrolysis.

2.2. Biochar Preparation

Processed biomass of *Solanum rostratum* was pyrolyzed at three target temperatures-400 °C, 500 °C, and 600 °C-to produce biochars with distinct surface characteristics relevant to sorption behavior. For each batch, approximately 35 g of oven-dried biomass was placed in lidded ceramic crucibles and pyrolyzed in a muffle furnace (SX2-4-10A, Shanghai Yiheng Instruments, China) under limited oxygen conditions. The temperature was raised at a constant rate of 10 °C min^{-1}, with a residence time of 4 h at the final temperature.

After naturally cooling to room temperature in a desiccator, the resulting biochars were gently ground and sieved to <0.25 mm for uniformity. Pyrolysis yield was calculated as the ratio of the dry biochar mass to the original dry biomass mass:

$$Yield(\%) = \frac{W_b}{W_0} \times 100 \quad (1)$$

where W_0 is the initial oven-dried biomass mass (g) and W_b is the mass of resulting biochar (g).

The biochars were designated as SRD400, SRD500, and SRD600 according to their pyrolysis temperatures. Uncharred biomass was referred to as SR. All samples were stored in sealed containers at room temperature until further characterization and incubation studies.

2.3. Soil Incubation Experiment

A controlled incubation experiment was conducted to assess the effects of *S. rostratum*–derived biochars on soil carbon mineralization and potential carbon stabilization through sorption-related mechanisms. Air-dried, sieved soil (<2 mm) was homogenized and placed into 250 mL glass incubation jars. Four treatments were established:

- SS: unamended soil (control);
- BC400: soil amended with SRD400 biochar at 10% (w/w);
- BC500: soil amended with SRD500 biochar at 10% (w/w);
- BC600: soil amended with SRD600 biochar at 10% (w/w).

Each treatment included four replicates. The biochar application rate of 10% (w/w) was selected to simulate a high-input scenario relevant to degraded lands or restoration contexts, enabling clearer observation of biochar–soil interactions and sorption-driven stabilization effects. Notably, the soils used originated from non-agricultural areas, ensuring ecological relevance without affecting arable productivity.

All jars were adjusted to 60% of water-holding capacity (WHC) and sealed with gas-permeable membranes to maintain aerobic conditions. Incubation was carried out in the dark at 25 ± 1 °C for 60 days. CO_2 emissions were measured at days 1, 3, 5, 7, 10, 15, 20, 30, 45, and 60 using an alkali absorption–acid titration method. At each sampling time point, NaOH traps were replaced, and captured CO_2 was titrated with standardized HCl to quantify cumulative carbon mineralization.

To quantify labile and stabilized carbon pools, cumulative CO_2 release was fitted to a two-pool first-order kinetic model:

$$M_t = C_l(1 - e^{-k_l t}) + C_s(1 - e^{-k_s t}) \quad (2)$$

where M_t is the cumulative mineralized carbon at time t; C_l and C_s represent the sizes of labile and stable carbon pools, and k_l and k_s are their respective decomposition rate constants. The proportion of stable carbon was calculated as:

$$StableC(\%) = \frac{C_s}{C_l + C_s} \times 100 \quad (3)$$

 doi:10.20944/preprints202511.1492.v1

Nonlinear regression fitting was performed using Origin to extract kinetic parameters, providing insights into the potential carbon stabilization efficacy of each biochar treatment.

2.4. Biochar Characterization and Physicochemical Properties

Biochars were comprehensively characterized to evaluate their sorption-relevant physicochemical properties and structural traits potentially influencing soil carbon stabilization.

pH and Water-Holding Capacity (WHC): Biochar pH was measured in a 1:20 (w/v) suspension with deionized water, shaken for 1 h and left to settle before reading with a digital pH meter (Mettler Toledo, Switzerland). WHC was determined by saturating 1 g of biochar in water for 24 h, draining for 20 h via pre-weighed filter paper, and calculating the difference between wet and oven-dried (105 °C, 12 h) masses.

Elemental Composition and Surface Morphology: Surface morphology and microstructure were observed using a field-emission scanning electron microscope (FESEM; GeminiSEM 500, ZEISS, Germany). Elemental composition was assessed via energy-dispersive X-ray spectroscopy (EDX) attached to the SEM, and expressed as both atomic and weight percentages.

Spectroscopic Analysis: Surface functional groups were identified by Fourier-transform infrared spectroscopy (FTIR; Nicolet iS50, Thermo Fisher, USA) over a 4000–400 cm^{-1} range. Aromaticity and carbon structure were evaluated using Raman spectroscopy (inVia, Renishaw, UK) with a 532 nm laser. X-ray diffraction (XRD; SmartLab, Rigaku, Japan) with Cu Kα radiation was used to detect crystalline and amorphous phases. Surface bonding environments and oxidation states were further characterized by X-ray photoelectron spectroscopy (XPS; ESCALAB 250Xi, Thermo Fisher, USA), with high-resolution peak deconvolution performed using XPSPEAK software.

Total Element Content and Ash: Total carbon (TC), total organic carbon (TOC), and total nitrogen (TN) contents were quantified using an elemental analyzer (Vario EL III, Elementar, Germany). TOC was measured after acid treatment to remove inorganic carbonates. Ash content was determined by combusting 1 g of biochar in a muffle furnace at 750 °C for 6 h.

These analyses enabled comparative evaluation of sorptive capacity, aromaticity, and functional group abundance across the SRD400, SRD500, and SRD600 biochars, offering mechanistic insight into their potential to adsorb and stabilize organic carbon in soil matrices.

2.5. Soil Physicochemical Analyses

At the end of the 60-day incubation, soil subsamples from each treatment were collected to assess the effects of biochar amendments on key physicochemical properties and carbon pool stability.

Elemental Composition and pH: Total carbon (TC) and total nitrogen (TN) contents were analyzed using an elemental analyzer (Vario EL III, Elementar, Germany). Total organic carbon (TOC) was determined by the potassium dichromate oxidation method with external heating. Soil pH was measured in a 1:2.5 (w/v) soil-to-deionized water suspension using a calibrated pH meter.

Moisture Content and Stable Carbon Fraction: Gravimetric soil moisture was calculated by oven-drying fresh soil at 105 °C for 24 h. The proportion of the stable carbon pool (StableC, %) was estimated using the kinetic model parameters (C_s) derived from the two-pool decomposition model described in Section 2.3.

These measurements provided a quantitative basis for evaluating how sorption-related stabilization and biochar–soil interactions influence carbon retention under different thermal biochar treatments.

2.6. Microbial Community Analysis

To elucidate microbial community responses and their potential roles in carbon stabilization following biochar amendment, soil samples from each treatment group (SS, BC400, BC500, and BC600) were collected after 60 days of incubation for microbial analysis.

 doi:10.20944/preprints202511.1492.v1

DNA Extraction and Sequencing: Total genomic DNA was extracted from 0.5 g of fresh soil using the FastDNA™ Spin Kit for Soil (MP Biomedicals, USA), following the manufacturer's instructions. DNA quality and quantity were assessed using a NanoDrop spectrophotometer and 1% agarose gel electrophoresis. The bacterial 16S rRNA gene (V3–V4 region) was amplified using primers 338F (5′-ACTCCTACGGGAGGCAGCAG-3′) and 806R (5′-GGACTACHVGGGTWTCTAAT-3′). Amplicons were purified, quantified, and pooled in equimolar ratios prior to sequencing on the Illumina MiSeq PE300 platform (Illumina, San Diego, USA).

Bioinformatics and Community Analysis: Raw reads were processed using QIIME2 (v2022.8). Paired-end reads were merged, quality-filtered, and denoised with DADA2 to generate amplicon sequence variants (ASVs). Taxonomic classification was performed against the SILVA 138.1 reference database.

Diversity Metrics and Functional Prediction: Alpha diversity indices (Chao1 richness, Shannon diversity, and Pielou evenness) and beta diversity (Bray–Curtis dissimilarity) were calculated and visualized via non-metric multidimensional scaling (NMDS) and principal coordinate analysis (PCoA) using the vegan and ggplot2 packages in R (v4.2.1). Potential microbial functional profiles were inferred using FAPROTAX. To evaluate community assembly processes, β-nearest taxon index (βNTI) and Raup–Crick dissimilarity based on Bray–Curtis (RC_bray) were calculated. Redundancy analysis (RDA) was used to examine relationships between microbial community structure and environmental variables.

These analyses enabled assessment of how biochar-driven sorption processes modulate microbial community structure and function, thereby contributing to carbon stabilization pathways.

2.7. Statistical Analysis

All data are presented as mean ± standard deviation (SD). Prior to analysis, assumptions of normality and homogeneity of variance were tested using the Shapiro–Wilk and Levene's tests, respectively, in R (v4.2.1). One-way analysis of variance (ANOVA) was used to evaluate treatment effects on soil carbon fractions, physicochemical parameters, and microbial diversity metrics.

When significant differences were detected ($p < 0.05$), Tukey's HSD test was applied for multiple comparisons under equal variance; otherwise, the Games–Howell test was employed. Pearson's correlation analysis was conducted to explore associations among biochar properties, soil carbon pools, and microbial indices.

Redundancy analysis (RDA) and variance inflation factor (VIF) diagnostics were performed using the vegan package in R to identify key environmental drivers of microbial community structure and soil carbon dynamics. All visualizations, including boxplots, CO_2 mineralization curves, heatmaps, and ordination plots, were generated using ggplot2 and related packages.

3. Results

3.1. Structural Evolution of Biochars Governing Adsorption Capacity

The surface structure and chemical composition of biochars directly shape their adsorption performance in soil environments. Morphological and spectroscopic characterization revealed temperature-dependent changes in the physical and chemical properties of *Solanum rostratum*-derived biochars (Figure 1), which underlie their potential to stabilize carbon through adsorption mechanisms.

 doi:10.20944/preprints202511.1492.v1

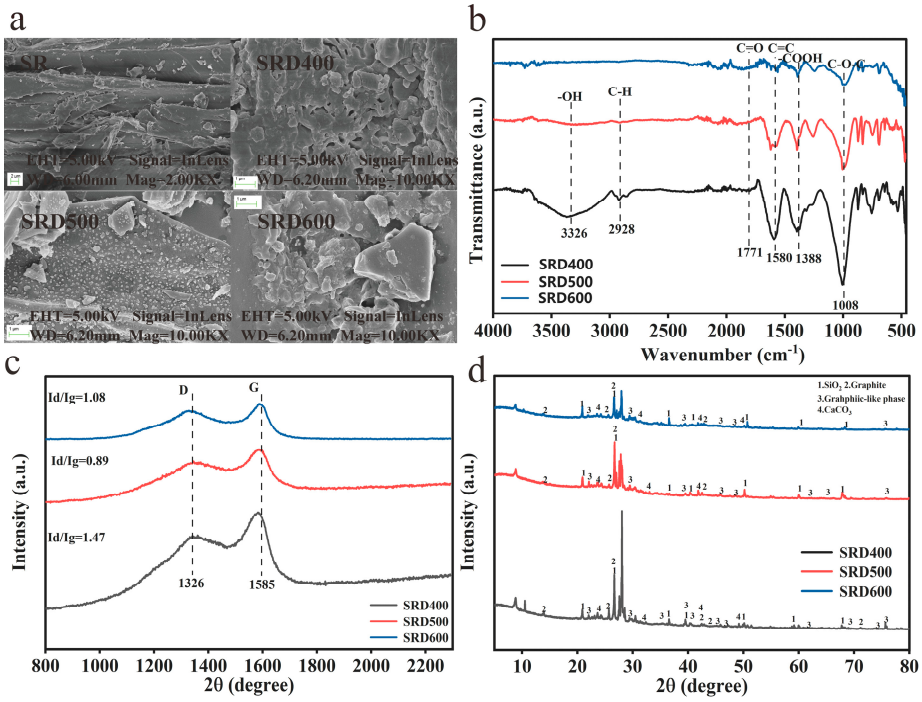

Figure 1. Morphological and structural characterization of *solanum rostratum*–derived biochars. (a) SEM images of raw material, SRD400, SRD500, and SRD600 showing morphological transformations during pyrolysis; (b) FTIR spectra of SRD400, SRD500, and SRD600 illustrating functional group changes with temperature; (c) Raman spectra displaying D and G bands and ID/IG ratios indicating carbon structural ordering; (d) XRD patterns reflecting the degree of aromatic condensation and crystallinity across pyrolysis treatments.

3.1.1. Surface Morphology and Porosity Development

Scanning electron microscopy (SEM) images (Figure 1a) showed progressive textural changes with increasing pyrolysis temperature. The raw biomass exhibited dense, fibrous tissues with limited porosity, while initial pore formation appeared at 400 °C. At 500 °C, pronounced pore enlargement and fragmentation were evident, exposing a more irregular surface—favorable for physical adsorption. Interestingly, at 600 °C, pore structures diminished, and surfaces became smoother, possibly due to structural collapse or sintering. These observations suggest that the 500 °C biochar likely offers the most favorable surface for sorption via micro- and mesopore development.

3.1.2. Functional Groups Relevant to Adsorption Sites

FTIR spectra (Figure 1b) revealed the thermal evolution of surface functional groups, including hydroxyl (–OH), carboxyl (–COOH), and carbonyl (C=O), which serve as active adsorption sites. These groups were abundant at 400 °C but declined sharply at higher temperatures, consistent with progressive deoxygenation. Such loss of polarity suggests a trade-off: lower-temperature biochars offer more chemical sorption potential, while higher-temperature materials exhibit greater physical stability and hydrophobicity.

Raman analysis (Figure 1c) confirmed carbon structural ordering, with ID/IG ratios indicating reduced disorder from 400 °C to 500 °C. At 600 °C, a slight increase in disorder suggested partial collapse of carbon domains. These structural patterns influence π–π interactions and van der Waals forces, both critical for adsorption of organic molecules or microbial metabolites.

3.1.3. Aromaticity and Crystallinity as Adsorption Scaffolds

 doi:10.20944/preprints202511.1492.v1

X-ray diffraction (XRD) patterns (Figure 1d) showed broadened peaks at 22–24° 2θ, indicative of amorphous carbon. The sharpening of these peaks with increasing temperature reflected growing aromatic condensation. This aromatization enhances biochar hydrophobicity and π-electron density, both of which strengthen sorptive interactions with nonpolar molecules and potentially facilitate microbial adhesion.

In summary, pyrolysis temperature modulates the trade-offs between biochar surface area, chemical functionality, and aromaticity—properties that collectively control adsorption capacity. Among the three pyrolysis treatments, SRD500 biochar likely achieves optimal balance for physical and chemical sorption, providing a favorable matrix for carbon stabilization and microbial colonization in subsequent processes.

3.2. Soil Carbon Stability and Mineralization Dynamics

3.2.1. Biochar-Derived Carbon Pool Distribution

The carbon pool composition of *Solanum rostratum*–derived biochars varied with pyrolysis temperature (Figure 2a). At 400 °C, the proportion of stable carbon (C sequestration) was ~32%, increasing slightly to ~34% at 500 and 600 °C. The oxidized carbon fraction remained low (2.7-4.6%), while the majority of carbon was thermally lost during pyrolysis. These results suggest that higher pyrolysis temperatures promoted stable carbon formation through aromatic condensation, enhancing the biochar's long-term carbon retention potential via adsorption and resistance to decomposition.

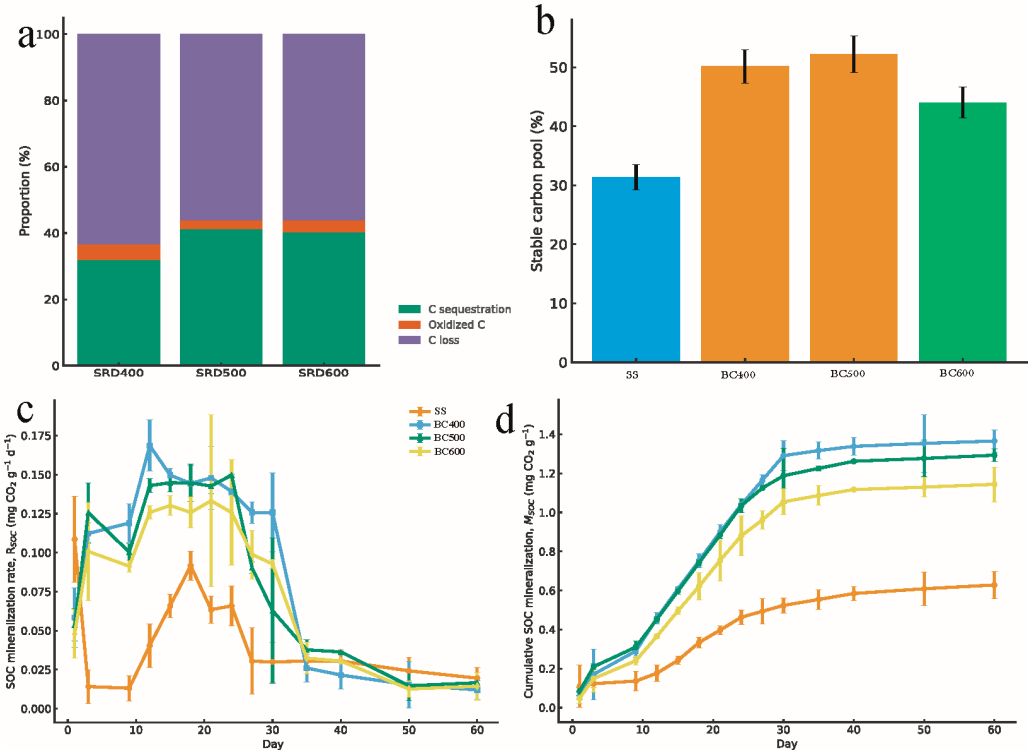

Figure 2. Carbon stability and mineralization dynamics following biochar application. (a) Carbon pool distribution in *Solanum rostratum*–derived biochars pyrolyzed at different temperatures, partitioned into carbon sequestration potential, oxidized carbon, and thermal loss fractions; (b) Proportion of the stable carbon pool (SCP) in soil amended with SRD biochars, estimated via a two-pool kinetic model; (c) Soil organic carbon mineralization rate (R_SOC) measured over a 60-day incubation period; (d) Cumulative CO_2-C release (M_SOC) indicating the total amount of carbon mineralized during incubation.

 doi:10.20944/preprints202511.1492.v1

3.2.2. Stability of Biochar-Amended Soil Carbon

After soil amendment, the proportion of the stable carbon pool (SCP) increased markedly compared to the control (SS), reaching 50.2%, 52.4%, and 44.3% under BC400, BC500, and BC600 treatments, respectively (Figure 2b). This enhancement in SCP reflects the contribution of biochar to stabilizing soil carbon pools. Notably, BC500 yielded the highest SCP, likely due to an optimal balance between surface functional groups and condensed aromatic structures, which favored carbon stabilization through sorptive interactions.

3.2.3. SOC Mineralization Kinetics

SOC mineralization rate (R_SOC) showed typical temporal dynamics across treatments (Figure 2c), with initial peaks between 10–20 days followed by a gradual decline. Biochar treatments significantly increased R_SOC relative to the control, with BC400 maintaining the highest rates. These results imply that low-temperature biochars retained labile carbon forms that stimulated microbial activity and co-metabolic decomposition.

Cumulative carbon mineralization (M_SOC) followed a similar trend (Figure 2d), with BC400 resulting in the highest cumulative CO_2 release (1.37 mg CO_2 g^{-1}), followed by BC500 and BC600. While increased mineralization may appear to reduce carbon persistence, it reflects an active microbial environment shaped by biochar adsorption dynamics, where labile and stabilized carbon coexist. This supports the dual role of biochar in enhancing both carbon turnover and sequestration.

3.2. Soil Carbon Stability and Mineralization Dynamics

3.2.1. Biochar-Derived Carbon Pool Distribution

The carbon pool composition of *Solanum rostratum*–derived biochars varied with pyrolysis temperature (Figure 2a). At 400 °C, the proportion of stable carbon (C sequestration) was ~32%, increasing slightly to ~34% at 500 and 600 °C. The oxidized carbon fraction remained low (2.7-4.6%), while the majority of carbon was thermally lost during pyrolysis. These results suggest that higher pyrolysis temperatures promoted stable carbon formation through aromatic condensation, enhancing the biochar's long-term carbon retention potential via adsorption and resistance to decomposition.

3.3. Soil Physicochemical Properties and Their Linkages to Carbon Stabilization

Biochar amendments significantly altered soil physicochemical properties, reinforcing their role in promoting adsorption-driven carbon stabilization mechanisms (Figure 3).

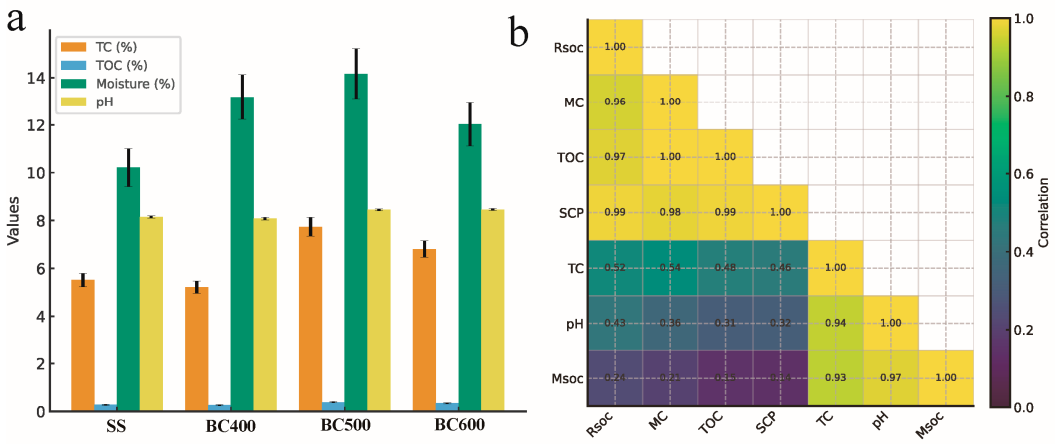

Figure 3. Soil physicochemical properties and their relationships with carbon stability. (a) Changes in total carbon (TC), total organic carbon (TOC), gravimetric moisture content, and pH in soils following the application

 doi:10.20944/preprints202511.1492.v1

of *Solanum rostratum*–derived biochars; (b) Pearson correlation heatmap showing relationships among TOC, pH, cumulative SOC mineralization (M_SOC), SOC mineralization rate (R_SOC), and the stable carbon pool proportion (SCP). Strong correlations underscore the role of soil physicochemical properties in driving carbon stabilization processes.

3.3.1. Changes in Soil TOC, pH, Moisture, and TC

As shown in Figure 3a, application of *Solanum rostratum*–derived biochars notably enhanced soil moisture content, especially in the BC400 and BC500 treatments, likely due to the porous structure and hydrophilicity of biochar surfaces. Soil pH remained within a slightly alkaline range (8.0–8.5), with marginal increases in BC500 and BC600. Total carbon (TC) increased markedly under BC500 and BC600, indicating improved carbon retention in soil. Similarly, TOC content followed the same trend, reaching the highest levels in BC500-treated soils.

The increase in TOC suggests that biochar not only contributes carbon directly but also adsorbs labile organic matter onto its surface, shielding it from microbial attack. This adsorption-mediated protection is particularly evident in intermediate-temperature biochars (e.g., BC500), which balance surface area and oxygen-containing functional groups favorable for sorption.

3.3.2. Correlation Analysis Supports Adsorption-Mediated Stability

The Pearson correlation heatmap (Figure 3b) revealed distinct patterns among key carbon pools and soil properties. The stable carbon pool (SCP) exhibited nearly perfect positive correlations with TOC ($r = 0.99$), moisture ($r = 0.98$), and SOC mineralization rate (R_SOC; $r = 0.99$), suggesting that SCP is closely linked to the adsorption and retention of labile organic matter. These variables clustered together, reflecting a coherent response to biochar-induced physicochemical changes.

In contrast, cumulative mineralization (M_SOC) correlated most strongly with pH ($r = 0.97$) and TC ($r = 0.93$), indicating that bulk carbon content and alkaline conditions may enhance overall decomposition but are less tightly linked to short-term sorptive stabilization.

These correlations collectively support the hypothesis that adsorption onto biochar surfaces plays a key role in carbon stabilization. Specifically, the co-variation of SCP with TOC and moisture implies that biochar facilitates physical protection and water-mediated adsorption of organic substrates, thus reducing their accessibility for microbial decomposition.

3.4. Biochar-Mediated Adsorptive Filtering of Microbial Communities

Amendment with *Solanum rostratum*–derived biochars resulted in measurable alterations in soil microbial community diversity and structure, consistent with an adsorptive filtering effect (Figure 4). Among alpha diversity indices, Pielou evenness showed a statistically significant decrease in BC400 compared to the control ($p=0.049$), suggesting a reduction in community uniformity under low-temperature biochar. In contrast, Chao1 richness and Shannon diversity remained relatively stable across treatments (Figures 4a–c), indicating that while species numbers were not drastically altered, community balance was modulated by biochar properties.

Multivariate ordinations reinforced the presence of treatment-specific microbial shifts. Principal Coordinates Analysis (PCoA, Figure 4d) and NMDS (Figure 4e) both showed clear clustering by biochar treatment, with BC500 and BC600 separating distinctly from the unamended soil (SS). These patterns reflect deterministic restructuring of bacterial communities as a function of pyrolysis temperature.

Such divergence is plausibly driven by the adsorptive filtering properties of biochar. As pyrolysis temperature increases, biochar surfaces evolve to exhibit more aromatic structures, hydrophobic domains, and porosity—features that facilitate physical adsorption of microbial cells and soluble nutrients. These surface characteristics may selectively retain or exclude microbial taxa, acting as physical–chemical barriers. Concurrently, modified soil environments (e.g., pH, TOC) create new ecological niches, reinforcing niche-based filtering. Together, these mechanisms support a model

 doi:10.20944/preprints202511.1492.v1

in which biochar not only modifies microbial habitats passively but actively filters community composition via adsorption-mediated selection.

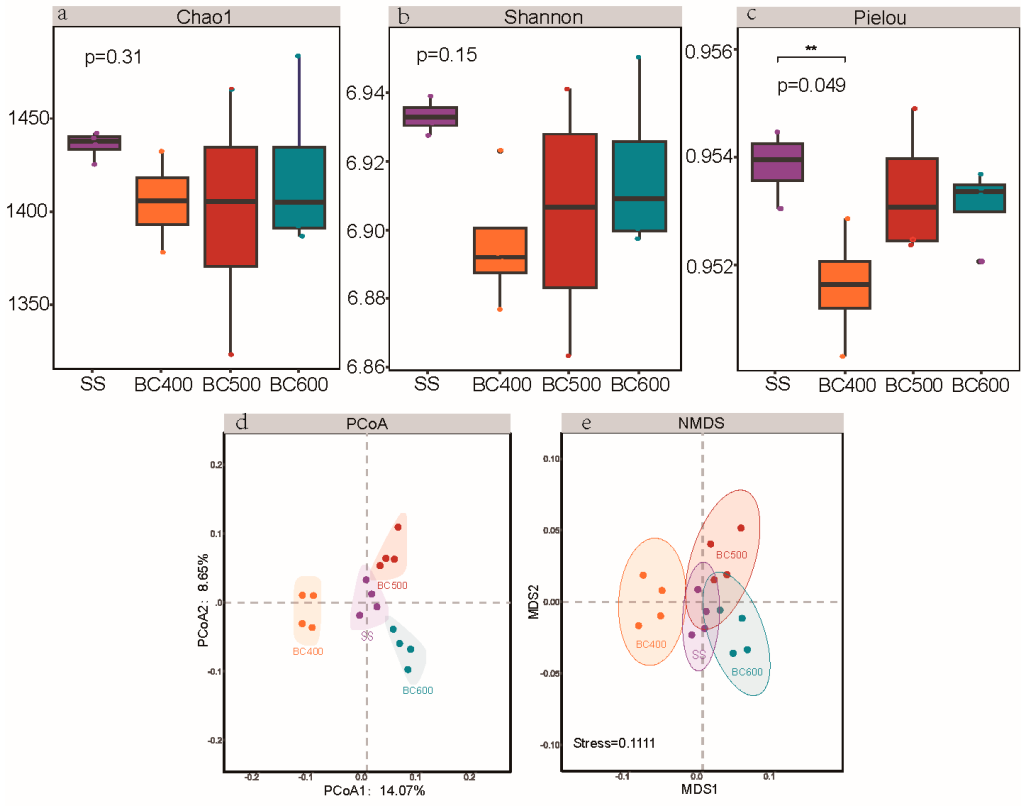

Figure 4. Microbial diversity and community structure in biochar-amended soils. (a–c) Alpha diversity metrics of bacterial communities under different treatments, including (a) Chao1 richness, (b) Shannon diversity, and (c) Pielou evenness. Pielou index revealed a significant decline in BC400 (p=0.049), indicating reduced evenness; (d) Principal Coordinates Analysis (PCoA) based on Bray–Curtis dissimilarity showing distinct microbial clustering by treatment; (e) Non-metric Multidimensional Scaling (NMDS) confirms divergence in community structure driven by biochar amendments. Both ordination analyses highlight the role of pyrolysis temperature in reshaping microbial assemblages.

3.5. Microbial Taxonomic Shifts and Functional Responses to Biochar Amendments

Solanum rostratum–derived biochar significantly influenced the taxonomic composition and predicted functional profiles of soil microbial communities (Figure 5). At the phylum level, Actinobacteriota, Proteobacteria, and Acidobacteriota dominated across treatments (Figure 5a, left). Biochar amendments—particularly at 500 °C and 600 °C-resulted in elevated relative abundances of Actinobacteriota and Chloroflexi, phyla known for their resilience to environmental stress and involvement in organic matter turnover. Conversely, Proteobacteria and Bacteroidota declined with increasing pyrolysis temperature, indicating a shift away from copiotrophic populations toward taxa more tolerant of nutrient-limited or sorptive environments.

 doi:10.20944/preprints202511.1492.v1

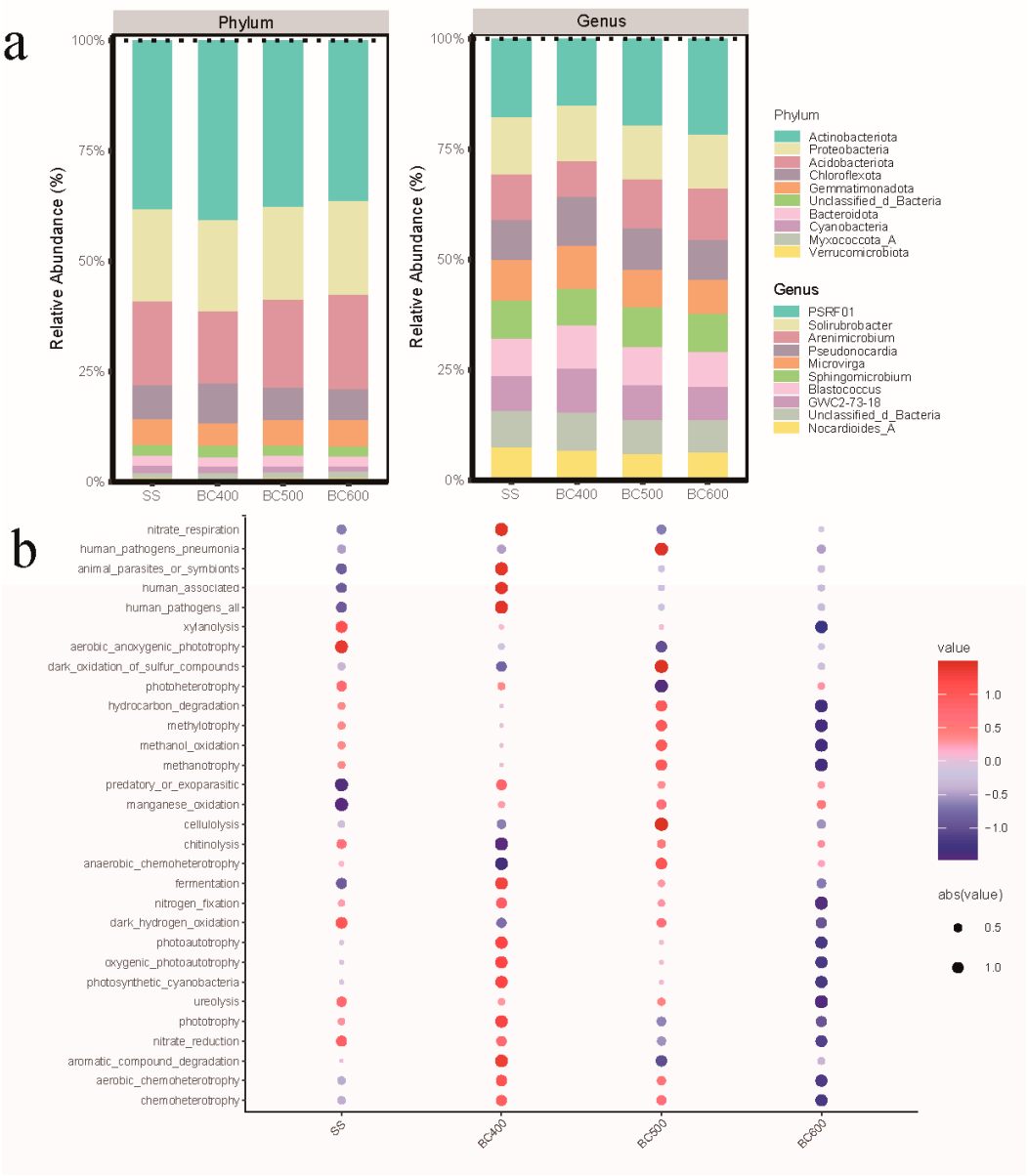

Figure 5. Microbial community composition and predicted functional pathways in response to biochar Amendments. (a) Relative abundances of dominant bacterial phyla (left) and genera (right) under different biochar treatments. Taxa associated with carbon metabolism and adsorption-resilience are highlighted; (b) Predicted microbial functional pathways inferred using FAPROTAX. Dot color represents functional enrichment (red) or depletion (blue), and size reflects effect magnitude. Pathways related to carbon cycling, nitrogen transformations, and environmental adaptation differ across treatments.

At the genus level (Figure 5a, right), biochar-amended soils exhibited enriched abundances of Solirubrobacter, Amycolatopsis, and Nocardioides_A, all of which have reported capacities for degrading aromatic compounds or thriving in adsorptive matrices. Notably, genera such as Sphingomonas and Blastococcus—associated with pollutant degradation and biofilm formation—were also favored by higher-temperature biochars. These trends align with the hypothesized role of biochar as a selective scaffold that filters microbial colonization based on surface chemistry and porosity.

Functional predictions based on FAPROTAX (Figure 5b) revealed further distinctions among treatments. Biochar application suppressed functions associated with nitrification and human-

 doi:10.20944/preprints202511.1492.v1

associated pathogens, while enriching carbon cycling-related pathways such as methanotrophy, methylotrophy, and aromatic compound degradation—particularly in BC500 and BC600. Enhanced functions like xylanolysis, cellulolysis, and aerobic chemoheterotrophy support the notion that biochar amendments modulate not just microbial identities but also ecological roles, likely through both physicochemical and substrate-mediated effects.

Collectively, these findings underscore that biochar-driven adsorption may influence microbial assemblages beyond diversity and structure, shaping broader ecosystem functions related to carbon stabilization and mineralization.

3.6. Environmental Determinants and Assembly Processes of Soil Microbial Communities

To elucidate how biochar-induced environmental changes shaped microbial community structure, we employed redundancy analysis (RDA), β-nearest taxon index (βNTI), and Raup–Crick Bray–Curtis metrics (RC_bray) (Figure 6). RDA revealed that stable carbon pool (SCP), pH, and soil moisture were the primary environmental drivers differentiating microbial assemblages across treatments (Figure 6c). SCP and moisture vectors pointed toward BC500 and BC400, suggesting that biochars produced at lower temperatures fostered environments conducive to stable carbon retention and microbial colonization. In contrast, BC600 showed a unique directional separation, potentially due to reduced labile substrates and altered sorption profiles.

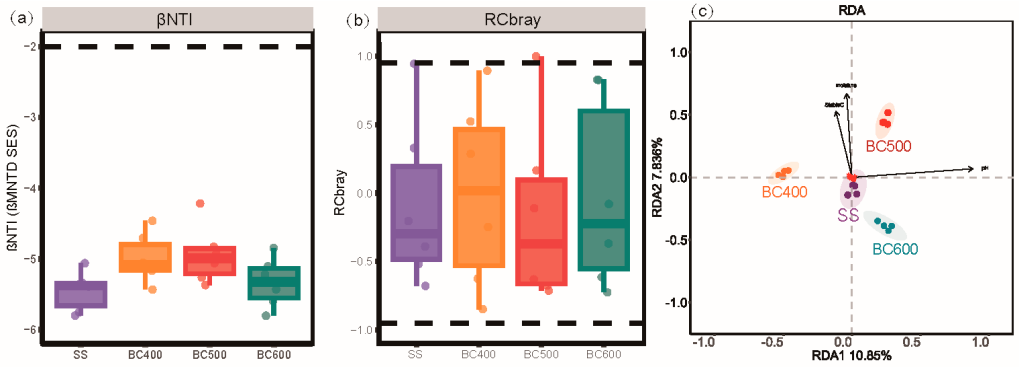

Figure 6. Environmental Drivers and Assembly Mechanisms of Microbial Communities. (a) β-nearest taxon index (βNTI) values across treatments, where |βNTI| > 2 indicates deterministic processes in community assembly; (b) Raup–Crick Bray–Curtis dissimilarity (RC_bray) quantifying deviations from null expectations and revealing niche versus stochastic contributions; c) Redundancy analysis (RDA) showing the influence of stable carbon pool (SCP), moisture, and pH on microbial community composition. Arrows denote direction and strength of environmental drivers.

βNTI values across all treatments were consistently below -2 (Figure 6a), indicating a strong signal of deterministic assembly dominated by homogeneous selection. The increasingly negative βNTI values with higher pyrolysis temperatures imply intensified environmental filtering—likely driven by shifts in surface chemistry, porosity, and redox buffering capacity of biochar particles.

Complementary RC_bray values (Figure 6b) hovered around zero or above in most treatments, further reinforcing that deterministic factors (rather than stochastic dispersal or ecological drift) governed microbial community structuring. Particularly in BC500 and BC600, RC_bray distributions widened, implying an increase in niche partitioning and sorptive stabilization.

Together, these findings support a conceptual model in which *Solanum rostratum*–derived biochar modulates microbial community assembly through its physicochemical properties—enhancing niche filtering and reducing stochastic variability via adsorption-mediated habitat selection.

 doi:10.20944/preprints202511.1492.v1

4. Discussion

4.1. Pyrolysis Temperature and Biochar Properties

Biochar's physicochemical attributes, including functional groups, porosity, and surface area, depend strongly on pyrolysis conditions. High-temperature pyrolysis (e.g. 500-800 °C) removes volatile components and oxygenated surface groups, yielding carbon-rich biochars with large BET surface areas and abundant micropores [29]. In contrast, low-temperature chars retain more labile, oxygen-containing functional groups and amorphous carbon (higher CEC and volatile content) [30]. Thus, increasing pyrolysis temperature generally increases biochar's specific surface area, porosity and pH (due to ash content), while decreasing polar surface functional groups (hydroxyl, carbonyl, carboxyl) [31]. For example, Barszcz et al. (2024) report that steam-activated biochars made at higher temperatures (~700-800 °C) exhibit greatly enhanced microporosity and surface area, whereas low-temperature biochars (300 °C) have more oxygenated functional groups and more graphitized carbon [32]. Overall, biochar's high surface area and multiscale pore structure are key to its adsorptive capacity [29].

4.2. Adsorption by Biochar: Surface Chemistry and Porosity

Biochar's porous surface and chemical functionality enable strong adsorption of organic compounds and nutrients [33]. Condensed aromatic carbon domains provide hydrophobic surface regions, while surface oxygen groups (-H, -COOH, etc.) enable hydrogen bonding and electrostatic attractions with polar molecules[29]. These diverse binding sites allow biochar to non-selectively sorb a wide range of organics (e.g. dissolved organic matter, pollutants) and inorganics. Crucially, biochar's hierarchical pore network creates microsites for adsorption: sub-nanometer micropores physically trap small molecules, while larger meso- and macropores (>2 nm) can accommodate enzymes, exoenzymes or small microbial cells. Tomczyk et al. (2020) note that biochar exhibits pores spanning micro- to macro-scales, with large "longitudinal" pores derived from biomass vascular structure [29]. The overall effect is a greatly expanded internal surface area. In short, high porosity and rich surface chemistry make biochar a high-capacity adsorbent [34].

By providing an abundance of adsorptive hotspots, biochar creates myriad microhabitats that can concentrate nutrients and organics [35]. For example, root exudates and DOC can become sorbed on biochar particles, leading to microregions of elevated substrate availability. Conversely, much labile C may be sequestered onto biochar pores, reducing bulk soil C availability (negative priming) [36]. In that study, added glucose was preferentially adsorbed and retained in biochar pore space, boosting microbial uptake but then locking dead microbial residues (necromass) inside biochar. Thus, biochar both stores labile C and protects it from rapid decomposition. The net result is that adsorbed C is stabilized: biochars effectively function as organo-mineral-like matrices where microbial necromass and organic compounds become occluded and shielded from decay [36].

4.3. Adsorptive Filtering of Microbial Communities

The adsorption properties of biochar also filter microbial communities by altering resource availability and habitat quality [37]. In biochar-amended soil, many soluble organics and nutrients become bound to biochar surfaces, creating niche patches of high and low resource density. Microorganisms colonizing biochar surfaces thus experience a different microenvironment than those in bulk soil: biochar pores can sustain biofilms and harbor slowly-diffusing substrates, while adjacent soil may be depleted of easily-mineralizable C [38]. In effect, biochar can concentrate certain labile resources (like root exudates) at its interface, making them accessible mainly to particle-associated microbes [36,39]. Those microbes must possess enzymes or survival strategies to exploit adsorbed organics. As a result, biochar often selects for taxa adapted to these niches. For example, oligotrophic or carbon-efficient bacteria and fungi that can utilize low concentrations of adsorbed C [36].

 doi:10.20944/preprints202511.1492.v1

This niche differentiation implies that biochar exerts a deterministic influence on community composition. Indeed, meta-analyses show that higher biochar doses reduce the importance of stochastic assembly, instead increasing homogeneous environmental selection (shared traits) among communitieslink.springer.com. Lei et al. (2023) found that with increasing biochar content, the fraction of community variance due to stochastic processes steadily declined, meaning that biochar led to more deterministic, niche-driven assembly [40]. Likewise, field trials report that after biochar amendment, beta-null-model analyses often show $|\beta NTI|>2$ and strong homogeneous selection (convergent traits) dominating community differences [41]. In practical terms, biochar creates habitat filters, through pH, moisture, and adsorbed substrates, that favor microbes with particular metabolic or stress-tolerance traits (niche specialists) over neutral, random colonizers [40].

4.4. Carbon Stabilization Mechanisms

Biochar's role in SOC stabilization combines physical and ecological processes. Physically, biochar's pores and surfaces adsorb organic matter (plant residues, DOC, microbial products), impeding its microbial access and diffusion. This leads to a negative priming effect: both native SOC and added substrates decompose more slowly in the presence of biochar (so biochar "saves" SOC) [36]. Experiments show that biochar-amended soils mineralize less native C than unamended controls, precisely because some C is trapped in biochar-associated organic matter pools [28]. In addition, biochar can occlude organic matter within soil aggregates and organo-mineral complexes: for example, soils often have a new class of "biochar-associated" SOC (adsorbed on biochar-mineral surfaces) that is more turnover-resistant (e.g. negative priming persists) [36].

Ecologically, biochar enhances microbial carbon use efficiency (CUE) and biomass. By providing protected niches and moderate substrates, biochar-fed microbes can grow more efficiently with less respiration (i.e. higher CUE). Biochar addition increased microbial biomass C and CUE, so that more of incoming C ended up in microbial biomass rather than CO_2. Importantly, when these microorganisms die, their necromass (amino-sugar residues) tends to accumulate in biochar pores. Kalu et al. traced ^13C-labelled glucose and showed that dead microbial biomass became sequestered inside biochar, raising microbial necromass carbon pools [36]. Similarly, Wang et al. (2025) report that biochar markedly enhanced microbial necromass carbon (especially bacterial necromass) in a saline soil, likely because the amended community structure promoted a stronger "microbial carbon pump" toward biomass production [42]. Thus, biochar helps convert labile inputs into stable microbial residues.

Together, these effects mean that biochar amplifies SOC stocks by shielding carbon from decomposition and by diverting more C into the long-lived fraction of microbial necromass. The combination of physical protection (adsorption, occlusion) and enhanced necromass formation under biochar is viewed as a key mechanism for long-term carbon stabilization [43].

4.5. Biochar-Modified Soil Environment and Community Outcomes

Beyond: adsorption, biochar alters soil abiotic conditions, further influencing which microbes persist. Its alkalinity often raises soil pH (liming effect), which in turn shifts microbial assembly toward neutrophilic taxa [29]. For example, many studies report that pH-hardware (liming) biochars suppress acidophiles and favor nitrifiers or other neutrophiles. Biochar's high surface area also increases soil cation exchange capacity and nutrient retention, making nutrients (e.g. NH_4^+, K^+, P) more available in microhabitats, which can benefit copiotrophs locally. Conversely, nutrient sorption by biochar can locally restrict availability for others [44]. Furthermore, biochar improves soil water retention due to its porous matrix (especially in coarse-textured soils), creating buffered microenvironments that allow moisture-sensitive microbes to survive drought periods longer [45]. These altered conditions (pH, moisture, nutrient adsorption) act as abiotic filters, reinforcing the trend toward deterministic community changes. In sum, biochar erects multiple niche filters

 doi:10.20944/preprints202511.1492.v1

(chemical and physical), so that microbial community assembly becomes strongly habitat-driven and predictable [38,40].

4.6. Implications

Biochar's efficacy in stabilizing soil carbon and shaping microbial communities is largely mediated by its adsorption characteristics. The interplay of high surface area, multiscale porosity, and reactive functional groups enables biochar to sequester organic substrates and water, creating heterogeneous niches. This promotes selective microbial colonization and deterministic assembly, increases microbial C use efficiency and necromass production, and ultimately results in greater SOC persistence. These adsorption-mediated mechanisms, from surface sorption to niche filtering, underlie many of the observed benefits of biochar amendments (carbon sequestration, pollutant immobilization, improved nutrient cycling), and are now substantiated by recent empirical and meta-analytic studies [40].

5. Conclusions

This study demonstrates that biochar derived from the invasive species *Solanum rostratum* and pyrolyzed at different temperatures exerts distinct influences on soil carbon stabilization and microbial ecology, primarily through adsorption-mediated processes. Biochars produced at intermediate temperatures (notably 500 °C) exhibited optimal structural features—aromatic carbon domains and preserved surface functionalities-that promoted both stable carbon pool formation and favorable microbial restructuring.

Our results show that adsorption is central to the dual role of biochar: it not only protects labile organic compounds from mineralization by immobilizing them on porous surfaces but also shapes microbial community assembly via niche filtering. This was reflected in reduced SOC mineralization rates, enlarged stable carbon pools, and deterministic microbial selection (e.g., elevated βNTI values). The enrichment of microbial taxa associated with carbon cycling and predicted functional pathways further supports the role of adsorptive filtering in regulating microbial metabolism and necromass contributions to long-term carbon retention.

These findings highlight the potential of adsorptive interactions as a key mechanism linking biochar's physicochemical properties to ecosystem-scale carbon outcomes. By integrating carbon dynamics with microbial ecological theory, our study provides mechanistic insights into how invasive-plant-derived biochars can be designed for maximal carbon sequestration. The results also underscore the broader applicability of adsorption-focused strategies in guiding sustainable biochar use on marginal or degraded soils under global change conditions.

Author Contributions: Conceptualization, L.S.; methodology, L.S., P.X., X.Z. and Z.G.; validation, X.Z. and Z.G.; formal analysis, L.S. and P.X.; investigation, L.S., P.X., X.Z. and Z.G.; resources, X.Z. and Z.G.; data curation, L.S. and P.X.; writing—original draft preparation, L.S. and P.X.; writing—review and editing, L.S., P.X., X.Z. and Z.G.; visualization, L.S. and P.X.; supervision, Z.G.; project administration, Z.G.; funding acquisition, Z.G. All authors have read and agreed to the published version of the manuscript.

Funding: This research was funded by CAS Key Laboratory of Forest Ecology and Silviculture, Institute of Applied Ecology, Chinese Academy of Sciences, grant number KLFES-2034.

Institutional Review Board Statement: Not applicable.

Informed Consent Statement: Not applicable.

Data Availability Statement: Data generated during this study are included in this paper; further information is available from the corresponding author upon request.

Acknowledgments: Sincere thanks to the reviewers of the article for their valuable comments and suggestions.

Conflicts of Interest: The authors declare no conflicts of interest.

 doi:10.20944/preprints202511.1492.v1

References

1. Stockmann, U.; Adams, M.A.; Crawford, J.W.; Field, D.J.; Henakaarchchi, N.; Jenkins, M.; Minasny, B.; McBratney, A.B.; Courcelles, V. de R. de; Singh, K.; Wheeler, I.; Abbott, L.; Angers, D.A.; Baldock, J.; Bird, M.; Brookes, P.C.; Chenu, C.; Jastrow, J.D.; Lal, R.; Lehmann, J.; O'Donnell, A.G.; Parton, W.J.; Whitehead, D.; Zimmermann, M. The knowns, known unknowns and unknowns of sequestration of soil organic carbon. *Agric. Ecosyst. Environ.* **2013**, 164, 80–99. https://doi.org/10.1016/j.agee.2012.10.001
2. Ghosh, S.; Divya, D.; Nath, A.; Yadav, V.S.; Singh, S.; Andleebajan, S.; Hansda, S.; Kumar, A. Carbon sequestration in agricultural soils: Strategies for climate change mitigation-A Review. *Int. J. Adv. Biochem. Res.* **2024**, *8*(12), 159–168. **https://doi.org/**10.33545/26174693.2024.v8.i12c.3087
3. Liang, Y.; Leifheit, E.F.; Lehmann, A.; Rillig, M.C. Soil organic carbon stabilization is influenced by microbial diversity and temperature. *Sci. Rep.* **2025**, *15*(1), 13990. https://doi.org/10.1038/s41598-025-98009-9
4. Blanco-Canqui, H. Biochar and soil physical properties. *Soil Sci. Soc. Am. J.* **2017**, *81*(4), 687–711. https://doi.org/10.2136/sssaj2017.01.0017
5. Varkolu, M.; Gundekari, S.; Omvesh; Palla, V.C.; Kumar, P.; Bhattacharjee, S.; Vinodkumar, T. Recent advances in biochar production, characterization, and environmental applications. *Catalysts* **2025**, *15*(3), 243. https://doi.org/10.3390/catal15030243
6. Fernando, T.; Fernando, D.; Gunatilake, S.; Zhang, X. Biochar-based contaminant removal: A tutorial on analytical quality assurance and best practices in batch sorption. *J. Chromatogr. Open* **2025**, *7*, 100219. https://doi.org/10.1016/j.jcoa.2025.100219
7. He, R.; Hui, K.; Zhang, X.; Yao, H. Insight into the role of the pore structure and surface functional groups in biochar on the adsorption of sulfamethoxazole from synthetic urine. *Appl. Sci.* **2024**, *14*(5), 1715. https://doi.org/10.3390/app14051715
8. Keiluweit, M.; Nico, P.S.; Johnson, M.G.; Kleber, M. Dynamic molecular structure of plant biomass-derived black carbon (biochar). *Environ. Sci. Technol.* **2010**, *44*(4), 1247–1253. https://doi.org/10.1021/es9031419
9. Dai, W.; Bao, Z.; Meng, J.; Chen, T.; Liang, X. Biochar makes soil organic carbon more labile, but its carbon sequestration potential remains large in an alternate wetting and drying paddy ecosystem. *Agronomy* **2025**, *15*(7), 1547. https://doi.org/10.3390/agronomy15071547
10. Du, J.; Gao, Q.; Sun, F.; Liu, B.; Jiao, Y.; Liu, Q. Agricultural soil microbiomes at the climate frontier: Nutrient-mediated adaptation strategies for sustainable farming. *Ecotoxicol. Environ. Saf.* **2025**, *295*, 118161. https://doi.org/10.1016/j.ecoenv.2025.118161
11. Ghorbani, M.; Amirahmadi, E.; Neugschwandtner, R.W.; Konvalina, P.; Kopecký, M.; Moudrý, J.; Perná, K.; Murindangabo, Y.T. The impact of pyrolysis temperature on biochar properties and its effects on soil hydrological properties. *Sustainability* **2022**, *14*(22), 14722. https://doi.org/10.3390/su142214722
12. Sathyabama, K.; Firdous, S. Effect of pyrolysis temperature on the physicochemical properties and structural characteristics of agricultural wastes-derived biochar. *ACS Omega* **2025**, *10*(33), 37013–37024. https://doi.org/10.1021/acsomega.5c00120
13. Conte, P.; Bertani, R.; Sgarbossa, P.; Bambina, P.; Schmidt, H.-P.; Raga, R.; Lo Papa, G.; Chillura Martino, D.F.; Lo Meo, P. Recent developments in understanding biochar's physical–chemistry. *Agronomy* **2021**, *11*(4), 0615. https://doi.org/10.3390/agronomy11040615
14. Singh, B.P.; Cowie, A.L.; Smernik, R.J. Biochar carbon stability in a clayey soil as a function of feedstock and pyrolysis temperature. *Environ. Sci. Technol.* **2012**, *46*(21), 11770–11778. https://doi.org/10.1021/es302545b
15. Ding, Y.; Liu, Y.; Liu, S.; Li, Z.; Tan, X.; Huang, X.; Zeng, G.; Zhou, L.; Zheng, B. Biochar to improve soil fertility. A review. *Agron. Sustain. Dev.* **2016**, *36*(2), 36. https://doi.org/10.1007/s13593-016-0372-z
16. Korai, S.K.; Korai, P.K.; Jaffar, M.A.; Qasim, M.; Younas, M.U.; Shabaan, M.; Zulfiqar, U.; Wang, X.; Artyszak, A. Leveraging biochar amendments to enhance food security and plant resilience under climate change. *Plants* **2025**, *14*(13), 1984. https://doi.org/10.3390/plants14131984
17. Zhu, X.; Chen, B.; Zhu, L.; Xing, B. Effects and mechanisms of biochar-microbe interactions in soil improvement and pollution remediation: A review. *Environ. Pollut.* **2017**, *227*, 98–115. https://doi.org/10.1016/j.envpol.2017.04.032

 doi:10.20944/preprints202511.1492.v1

18. Liu, C.; Ye, J.; Lin, Y.; Wu, X.; Shu, W.; Wang, Y. Effects of co-application of biochar and nitrogen fertilizer on soil properties and microbial communities in tea plantation. *Agriculture* **2025**, *15*(18), 1941. https://doi.org/10.3390/agriculture15181941
19. Mukherjee, S.; Sarkar, B.; Aralappanavar, V.K.; Mukhopadhyay, R.; Basak, B.B.; Srivastava, P.; Marchut-Mikołajczyk, O.; Bhatnagar, A.; Semple, K.T.; Bolan, N. Biochar-microorganism interactions for organic pollutant remediation: challenges and perspectives. *Environ. Pollut.* **2022**, *308*, 119609. https://doi.org/10.1016/j.envpol.2022.119609
20. Dini-Andreote, F.; Stegen, J.C.; van Elsas, J.D.; Salles, J.F. Disentangling Mechanisms That mediate the balance between stochastic and deterministic processes in microbial succession. *Proc. Natl. Acad. Sci. USA* **2015**, *112*(11), E1326–E1332. https://doi.org/10.1073/pnas.1414261112
21. Stegen, J.C.; Lin, X.; Fredrickson, J.K.; Chen, X.; Kennedy, D.W.; Murray, C.J.; Rockhold, M.L.; Konopka, A. Quantifying community assembly processes and identifying features that impose them. *ISME J.* **2013**, *7*(11), 2069–2079. https://doi.org/10.1038/ismej.2013.93
22. Du, M.; Xue, P.; Minasny, B.; McBratney, A.; Tang, Y. Soil bacterial, fungal, and protistan assembly processes across a 1300 km climate and land-use transect. *CATENA* **2026**, *262*, 109609. https://doi.org/10.1016/j.catena.2025.109609
23. Ozuzu, S.A.; Hussain, R.S.A.; Kuchkarova, N.; Fidelis, G.D.; Zhou, S.; Habumugisha, T.; Shao, H. Buffalo-bur (*Solanum rostratum* Dunal) invasiveness, bioactivities, and utilization: a review. *PeerJ* **2024**, *12*, e17112. https://doi.org/10.7717/peerj.17112
24. Abu-Nassar, J.; Gal, S.; Shtein, I.; Distelfeld, A.; Matzrafi, M. Functional leaf anatomy of the invasive weed *Solanum rostratum* Dunal. *Weed Res.* **2022**, *62*(2), 172–180. https://doi.org/10.1111/wre.12527
25. Woolf, D.; Amonette, J.E.; Street-Perrott, F.A.; Lehmann, J.; Joseph, S. Sustainable biochar to mitigate global climate change. *Nat. Commun.* **2010**, *1*, 56. https://doi.org/10.1038/ncomms1053
26. Ma, R.; Wu, X.; Liu, Z.; Yi, Q.; Xu, M.; Zheng, J.; Bian, R.; Zhang, X.; Pan, G. Biochar improves soil organic carbon stability by shaping the microbial community structures at different soil depths four years after an incorporation in a farmland soil. *Curr. Res. Environ. Sustain.* **2023**, *5*, 100214. https://doi.org/10.1016/j.crsust.2023.100214
27. Zhang, H.; Ma, T.; Wang, L.; Yu, X.; Zhao, X.; Gao, W.; Van Zwieten, L.; Singh, B.P.; Li, G.; Lin, Q.; Chadwick, D.R.; Lu, S.; Xu, J.; Luo, Y.; Jones, D.L.; Jeewani, P.H. Distinct biophysical and chemical mechanisms governing sucrose mineralization and soil organic carbon priming in biochar amended soils: evidence from 10 years of field studies. *Biochar* **2024**, *6*(1), 52. https://doi.org/10.1007/s42773-024-00327-0
28. Zimmerman, A.R.; Gao, B.; Ahn, M.-Y. Positive and negative carbon mineralization priming effects among a variety of biochar-amended soils. *Soil Biol. Biochem.* **2011**, *43*(6), 1169–1179. https://doi.org/10.1016/j.soilbio.2011.02.005
29. Tomczyk, A.; Sokołowska, Z.; Boguta, P. Biochar physicochemical properties: pyrolysis temperature and feedstock kind effects. *Rev. Environ. Sci. Biotechnol.* **2020**, *19*(1), 191–215. https://doi.org/10.1007/s11157-020-09523-3
30. de Oliveira Paiva, I.; de Morais, E.G.; Jindo, K.; Silva, C.A. Biochar N content, pools and aromaticity as affected by feedstock and pyrolysis temperature. *Waste Biomass Valor.* **2024**, *15*(6), 3599–3619. https://doi.org/10.1007/s12649-023-02415-x
31. Almutairi, A.A.; Ahmad, M.; Rafique, M.I.; Al-Wabel, M.I. Variations in composition and stability of biochars derived from different feedstock types at varying pyrolysis temperature. *J. Saudi Soc. Agric. Sci.* **2023**, *22*(1), 25–34. https://doi.org/10.1016/j.jssas.2022.05.005
32. Barszcz, W.; Łożyńska, M.; Molenda, J. Impact of pyrolysis process conditions on the structure of biochar obtained from apple waste. *Sci. Rep.* **2024**, *14*(1), 10501. https://doi.org/10.1038/s41598-024-61394-8
33. Dong, X.; Chu, Y.; Tong, Z.; Sun, M.; Meng, D.; Yi, X.; Gao, T.; Wang, M.; Duan, J. Mechanisms of adsorption and functionalization of biochar for pesticides: a review. *Ecotoxicol. Environ. Saf.* **2024**, *272*, 116019. https://doi.org/10.1016/j.ecoenv.2024.116019
34. Jagadeesh, N.; Sundaram, B. Adsorption of pollutants from wastewater by biochar: a review. *J. Hazard. Mater. Adv.* **2023**, *9*, 100226. https://doi.org/10.1016/j.hazadv.2022.100226

 doi:10.20944/preprints202511.1492.v1

35. Tang, K.H. Biochar amendments for soil restoration: impacts on nutrient dynamics and microbial activity. *Environments* **2025**, *12*(11), 425. https://doi.org/10.3390/environments12110425
36. Kalu, S.; Seppänen, A.; Mganga, K.Z.; Sietiö, O.-M.; Glaser, B.; Karhu, K. Biochar reduced the mineralization of native and added soil organic carbon: evidence of negative priming and enhanced microbial carbon use efficiency. *Biochar* **2024**, *6*(1), 7. https://doi.org/10.1007/s42773-023-00294-y
37. Wang, C.; Chen, D.; Shen, J.; Yuan, Q.; Fan, F.; Wei, W.; Li, Y.; Wu, J. Biochar alters soil microbial communities and potential functions 3–4 years after amendment in a double rice cropping system. *Agric. Ecosyst. Environ.* **2021**, *311*, 107291. https://doi.org/10.1016/j.agee.2020.107291
38. Palansooriya, K.N.; Wong, J.T.F.; Hashimoto, Y.; Huang, L.; Rinklebe, J.; Chang, S.X.; Bolan, N.; Wang, H.; Ok, Y.S. Response of microbial communities to biochar-amended soils: a critical review. *Biochar* **2019**, *1*(1), 3–22. https://doi.org/10.1007/s42773-019-00009-2
39. Bhatt, B.; Gupta, S.K.; Mukherjee, S.; Kumar, R. A comprehensive review on biochar against plant pathogens: current state-of-the-art and future research perspectives. *Heliyon* **2024**, *10*(17), e37204. https://doi.org/10.1016/j.heliyon.2024.e37204
40. Lei, C.; Lu, T.; Qian, H.; Liu, Y. Machine learning models reveal how biochar amendment affects soil microbial communities. *Biochar* **2023**, *5*(1), 89. https://doi.org/10.1007/s42773-023-00291-1
41. Huber, P.; Metz, S.; Unrein, F.; Mayora, G.; Sarmento, H.; Devercelli, M. Environmental heterogeneity determines the ecological processes that govern bacterial metacommunity assembly in a floodplain river system. *ISME J.* **2020**, *14*(12), 2951–2966. https://doi.org/10.1038/s41396-020-0723-2
42. Wang, Y.; Gao, Y.; Zheng, H.; Wang, R.; Ge, Z.; Miao, Z. Biochar enhances soil organic carbon by stabilizing microbial necromass carbon in saline–alkaline topsoil. *Agronomy* **2025**, *15*(11), 2472. https://doi.org/10.3390/agronomy15112472
43. Lehmann, J.; Kleber, M. The contentious nature of soil organic matter. *Nature* **2015**, *528*(7580), 60–68. https://doi.org/10.1038/nature16069
44. Hossain, M.Z.; Bahar, M.M.; Sarkar, B.; Donne, S.W.; Ok, Y.S.; Palansooriya, K.N.; Kirkham, M.B.; Chowdhury, S.; Bolan, N. Biochar and its importance on nutrient dynamics in soil and plant. *Biochar* **2020**, *2*(4), 379–420. https://doi.org/10.1007/s42773-020-00065-z
45. Jia, A.; Song, X.; Li, S.; Liu, Z.; Liu, X.; Han, Z.; Gao, H.; Gao, Q.; Zha, Y.; Liu, Y.; Wu, X.; Wang, G. Biochar enhances soil hydrological function by improving the pore structure of saline soil. *Agric. Water Manag.* **2024**, *306*, 109170. https://doi.org/10.1016/j.agwat.2024.109170